Integrated Control of Internal Boundaries and Signal Timing at An Isolated Intersection for Lane-free Traffic of CAVs

Peng Yang, Xufeng Jin, Yonghui Hu, Yibing Wang, Mingming Zhao, Markos Papageorgiou, Jingqiu Guo*

***Abstract*—Urban traffic signal timing separates incompatible traffic flows in time, but normally cannot intervene in the utilization of road resources when the bi-directional (e.g. east and west bound) traffic demands are much unbalanced, because such demands receive the same right of way. A novel traffic control measure called internal boundary control (IBC) was recently proposed to address a similar concern on freeways for lane-free traffic of fully connected automated vehicles (CAVs). This paper applies the idea of IBC to maximize the utilization of intersection resources for improved urban traffic efficiency. The paper focuses on the joint optimization of roads' internal boundaries and signal timing for an isolated intersection in the paradigm of lane-free traffic of CAVs. The optimization problem is formulated as a binary-mixed-integer-quadratic-programing problem. The results show that the joint optimization has a potential of significantly improving traffic situations at an intersection, typically those intractable via signal timing optimization alone.**

I. Introduction

Signal timing at intersections has been studied and applied for a long time to improve urban traffic efficiency[1] [2]. It aims to allocate the entire intersection capacity temporally and provides the right of way to incompatible/antagonistic traffic streams in different phases of a cycle time. On the other hand, signal timing typically serves compatible bi-directional traffic streams (e.g. east-bound and west-bound) in the same signal phases. Therefore, road resources are equally assigned for traffic in the opposite directions, regardless whether the bi-directional demands are comparable or unbalanced. Thus, in case of unbalanced traffic demands, it happens that the traffic demand in one direction is not fully accommodated but there is spare capacity in the opposite direction.

Clearly, the above problem is related to the lane setting or road resource assignment, and goes beyond the scope of conventional traffic signal timing. Nevertheless, relevant efforts have been made over the past decades via the concept of reversible lanes. Specifically, reversible roadways have been considered to address a variety of needs [3], including special event management [4], emergency evacuation [5], and unbalanced travel demand during peak periods [6] [7].

With respect to urban intersections, reversible lanes are applied in the form of variable guidance lanes to accommodate the unbalanced bi-direction mobility and also tackle the imbalance of through and left-turning traffic. Collaborative optimization on variable guidance lanes and signal timing were studied in the past few years. Focusing on traffic in one direction, [8] considered the optimization of the changeable lane usage (for through or left-turning traffic) together with signal timing. [9] furthermore studied the possibility of taking the bi-directional traffic as a whole to cope with the collaborative optimization. [10] proposed a stochastic optimal model to improve the robustness of lane allocation.

The essence of applying reversal or variable guidance lanes is to transfer the redundant capacity in/for the uncongested direction/unsaturated traffic stream to the congested direction/quasi-saturated traffic stream in a "dynamic" manner. The aforementioned studies [8-10] address the "lane based" traffic mode, with the following limitations: (1) each reversible lane re-setting requires substantial clearance time for safety reasons, resulting in a waste of time and space resources; (2) reversible lanes need to be long enough to avoid forming weaving zones and causing traffic congestion; (3) traditional reversible lane operation takes a lane as the unit for space allocation, restricting the operating granularity in space.

A novel concept "TrafficFluid" was recently proposed for traffic flow of connected automated vehicles (CAVs) [11]. One typical feature of TrafficFluid is lane-free traffic, that is, CAVS are not restricted to the fixed traffic lanes, but can drive anywhere on the 2-D surface of the road with enough inter-vehicle spacing for safety. Following the concept of TrafficFluid, a novel traffic control measure of internal boundary control (IBC) has been proposed for lane-free traffic of CAVS on freeways [12]. The main idea of IBC is as follows: the currently rigid boundary between the bi-directional traffic can be softened for the lane-free traffic of CAVs. Thus, the resulting virtual internal boundary can be regulated by a roadside controller in real-time to respond to the unbalanced bi-directional traffic flows. In other words, the bi-directional road capacity can be shared between the two opposite directions according to their respective demands, and the

This work was supported in part by the National Natural Science Foundation of China (project number: 52272315), the Provincial Key R&D Program of Zhejiang (project number: 2021C01012; 2022C01129), and the R&D Program of the Zhejiang Communications Investment Group Co. Ltd. (project number: 202309).

P. Yang, X. Jin, Y. Hu and Y. Wang are with the Institute of Intelligent Transportation Systems, Zhejiang University,310058 Hangzhou, China (e-mail: wangyibing@zju.edu.cn)

M. Zhao is with the State Key Laboratory of Integrated Services Networks, Xidian University, Xi'an 710071, China and Hangzhou Institute of Technology, Xidian University, Hangzhou 311200, China. (e-mail: zhaomingming@xidian.edu.cn)

M. Papageorgiou is with the Dynamic Systems and Simulation Laboratory, Technical University of Crete, 73100, Chania, Greece (e-mail: mpapageorgiou@tuc.gr)

Jingqiu Guo is with the Key Laboratory of Road and Traffic Engineering of the Ministry of Education, Tongji University, Shanghai 201804, China (e-mail: guojingqiu@hotmail.com)

assignment can be managed in real-time to maximize road space utilization for improved traffic efficiency.

[12] first formulated IBC as a convex quadratic programing problem and demonstrated its performance for simple freeway scenarios. Later, Linear Quadratic regulators [13] and overlapping decentralized control schemes [14] were employed to implement IBC more practically on freeways. [15] combined ramp metering and IBC for improved traffic control results that ramp metering or IBC alone cannot achieve.

The above studies show the profound potential of IBC in better utilizing the existing infrastructure and improving traffic efficiency on freeways. However, the potential of IBC in urban traffic control is still unknown. This paper studies the coordinated control of internal boundaries and signal timing at an isolated intersection with unbalanced traffic demands in the lane-free paradigm of CAVs. To discover the essence of IBC for urban traffic flow management, two issues are of particular interest for this paper: (1) how much can signal control efficiency be improved via IBC; and (2) under what circumstances.

Signal timing optimization allocates the road capacity temporally via phase timing to address unbalanced incompatible traffic demands in the incompatible directions, while IBC can be applied to assign the road capacity spatially to deal with unbalanced compatible bi-directional traffic demands that share the same signal phases. The integration of IBC and signal timing is formulated as a binary-mixed-integer-quadratic-programing problem based on the store-and-forward model, and solved by the standard branch-and-bound technique in this paper. The obtained results show that the integrated control can better deal with traffic situations at an intersection, particularly those intractable by signal timing optimization or IBC alone.

The remainder of the paper is organized as follows: Section II introduces the problem statement. Section III formulates the joint optimization problem as a binary-mixed-integer-quadratic-programming problem. The study results are presented in Section IV. Section V concludes this paper.

II. Problem Statement

Fig. 1 shows an isolated intersection with the through movement in each direction. The considered traffic environment involves only connected automated vehicles (CAVs) high levels, where CAVs' states are all accessible for the intersection controller unit (ICU) and all CAVs' motions are fully controllable in real-time. As shown in Fig. 1, the ICU regulates the intersection's signal timings and the internal boundary of each road linked to the intersection so as to optimize the traffic flow efficiency. For simplicity, the left-turning traffic is not considered and the signal cycle is assumed fixed in this study.

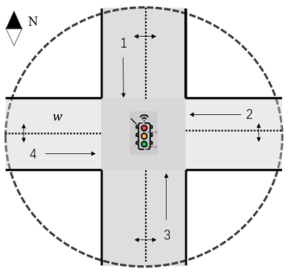

Fig. 1. The considered intersection.

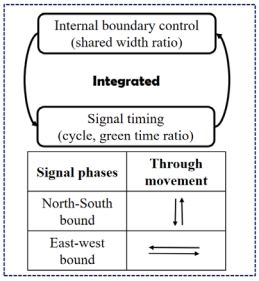

Fig. 2. The framework of the integrated control with intersection controller unit.

It is displayed in Fig. 1 that four traffic streams towards the intersection are considered in this work, each indicated by $i \in I = \{1,2,3,4\}$. The core of ICU is a joint optimization model that addresses both signal timing optimization and internal boundary control. The road resources are allocated temporally via signal timing optimization, and spatially via IBC.

III. Mathematical Formulation

A. Basic Settings

The store-and-forward model is employed in this paper to model traffic dynamics in each approach to the intersection, with a time step T of 5 seconds. The signal cycle C is fixed at 60 seconds, and each cycle is split into a number of time steps each of 5 seconds. The signal timing is optimized every time step, while IBC is conducted once per cycle.

To facilitate the formulation of the joint optimization problem, the following is assumed without loss of generality:

(1) once the traffic light turns to green, the queue of CAVs is dissolved at the saturation rate without the start loss;

(2) an increase (decrease) in the width of an approach leads to an increase (decrease) in the capacity of the approach, i.e. the saturation flow of the approach is proportional to its width, see also [11] [15] for more details.

B. Signal Timing Model

Since the cycle length is fixed, we focus on the optimization of the effective green times for all approaches, with the upper and lower bounds of the green times considered.

$$g_{min} \le T \cdot \sum_{n=1}^{N} \delta_{i,m,n} \le g_{max}, \ \forall i,m \quad (1)$$

where $g_{min} = 2 * T = 10s$, $g_{max} = 50s$, $\delta_{i,m,n}$ is a binary variable for the signal status in approach i at time step n of the m-th signal cycle. In other words, $\delta_{i,m,n}$ addresses the time instant $(m-1)C + nT$. That $\delta_{i,m,n} = 1$ means the traffic light is green, $\delta_{i,m,n} = 0$ means that traffic light is red. Given an approach i and a cycle m, $\delta_{i,m,n}$ changes only once between 0 and 1 within the cycle.

The equations (2) - (5) represent the basic phase constraints, with reference to Fig. 1,

$$\delta_{1,m,n} = \delta_{3,m,n} \quad (2)$$
$$\delta_{2,m,n} = \delta_{4,m,n} \quad (3)$$
$$\delta_{1,m,n} + \delta_{2,m,n} = 1 \quad (4)$$
$$T \cdot \sum_{n=1}^{N} (\delta_{i,m,n} + \delta_{i',m,n}) = C, \ \forall m, i \in \{1,3\}, \ i' \in \{2,4\} \quad (5)$$

These equations set the fundamental rules for traffic at a signalized intersection to avoid conflicts between traffic in opposing approaches. The cycle time is spilt into two phases, and one green signal phase must be activated at any time, assuming that the very short all red periods are negligible.

$$\delta_{1,m,0} = \delta_{3,m,0} = 1 \quad (6)$$
$$\delta_{2,m,0} = \delta_{4,m,0} = 0 \quad (7)$$
$$if \ \delta_{2,m,n-1} = \delta_{4,m,n-1} = 1, \ \delta_{2,m,n} = \delta_{4,m,n} = 1 \quad (8)$$

Equations (6) - (8) set the phase sequence constraints. It is stipulated with (6) and (7) that the start phases for approaches 1/2 and 3/4 (Fig. 1) are green/red. In each cycle, a phase change occurs only once, and this is secured with (8), i.e. the green phases start in approaches 1 and 3, and once approaches 1 and 3 switch to red and approaches 2 and 4 are given the right of way, this keeps until the end of the cycle.

C. Internal Boundaries Control Model

In the paradigm of the lane-free traffic of CAVs, CAVs are not necessarily bound to fixed lanes as in the conventional traffic, but may drive anywhere on the 2-D surface of the road, respecting the road boundaries, of course. Approaches 1 & 3 or Approaches 2 & 4 in Fig. 1 that occupy the same channel share the road resources (road width) to meet the possibly unbalanced traffic demands in the opposite directions. With reference to Fig. 1,

$$w_{1,m} + w_{3,m} \leq 1 \tag{9}$$

$$w_{2,m} + w_{4,m} \leq 1 \tag{10}$$

where $w_{\mathrm{i},m}, i = 1,2,3,4$ are the space shared ratios of approach i at signal cycle m. Note that these ratios are tuned at the frequency of a cycle, and hence not related to model step index n as done with $\delta_{i,m,n}$ previously introduced.

Consider the smoothness of the IBC, $w_{\mathrm{i},m}$ should change gradually in a step-by-step manner, i.e.

$$0 < w_{min} \leq w_{i,m} \leq w_{max} \leq 1 \tag{11}$$

$$\left|w_{i,m} - w_{i,m-1}\right| \leq w_0 \tag{12}$$

The time-delay issue is considered for the lane-based traffic with the physical reversible lane separation to ensure safety [16]. The same is also true for the lane-free urban IBC. The attention should be given only to the traffic direction that is being widened, while the direction that is restricted/narrowed should promptly adopt the determined smaller width. In this work, the above idea is implemented via the following:

$$w_{i,m}^{c} = \min\{w_{i,m}, w_{i,m-1}\} \tag{13}$$

D. Store-and-forward Model of Vehicle Traffic

The model can be expressed as follows:

$$L_{i,m,n+1} = L_{i,m,n} + T(q_{i,m,n}^{in} - q_{i,m,n}^{out}) \tag{14}$$

$$q_{i,m,n}^{out} = min\{q_{i,m,n}^{in} + \frac{L_{i,m,n}}{T},\ q_{i,m,n}^{cap}\} \tag{15}$$

$$q_{i,m,n}^{cap} = \mathrm{Q} w_{i,m}^{c} \delta_{i,m,n} \tag{16}$$

where $L_{i,m,n},\ i = 1,2,3,4$ denotes the vehicular queue length at the intersection in approach i at cycle m in step n, $q_{i,m,n}^{in}, i = 1,2,3,4$ the traffic demand in approach i at cycle m in step n, $q_{i,m,n}^{out}, i = 1,2,3,4$ the outflow of approach i at cycle m in step n, $q_{i,m,n}^{cap}, i = 1,2,3,4$ the flow capacity of approach i at cycle m in step n, which is not constant because of $w_{i,m}^{c}$.

Q represents the total capacity of the intersection. Assume that the intersection is a square, so Q applies to Approaches 1 & 3 and Approaches 2 & 4 as well. When Approaches 1 & 3 or Approaches 2 & 4 enjoy the right of way, they share the total capacity Q. (14) formulates the queueing model, (15) delivers the outflow that is determined with the demand and the supply, and (16) determines approach i's outflow capacity with the total capacity Q, the signal status $\delta_{i,m,n}$ and road width ratio $w_{i,m}^{c}$.

E. The Treatment of Nonlinear Inequality Constraints

This paper intends to deal with the joint optimization of signal timing and internal boundaries for lane-free CAV traffic at an isolated intersection. Except for formulae (13), (15), and (16), relations in sections B-D are linear. In order to formulate the aimed task as a quadratic programming problem, the nonlinear formulae (13), (15), and (16) need to be "linearized".

Firstly, (13) can be replaced with the following inequalities:

$$w_{i,m}^{c} \leq w_{i,m} \tag{17}$$

$$w_{i,m}^{c} \geq w_{i,m} - D(1 - u_{i,m,n,1}) \tag{18}$$

$$w_{i,m}^{c} \leq w_{i,m-1} \tag{19}$$

$$w_{i,m}^{c} \geq w_{i,m-1} - D(1 - u_{i,m,n,2}) \tag{20}$$

$$u_{i,m,n,1} + u_{i,m,n,2} \geq 1 \tag{21}$$

$$u_{i,m,n,1}, u_{i,m,n,2} \in \{0,1\} \tag{22}$$

where D is a very large positive constant, and $u_{i,m,n,1}$, $u_{i,m,n,2}$ are binary variables.

The same idea applies to (15) as well:

$$q_{\mathrm{i,m,n}}^{out} \leq q_{i,m,n}^{in} + \frac{\mathrm{L}_{i,m,n}}{T} \tag{23}$$

$$q_{i,m,n}^{out} \geq q_{i,m,n}^{in} + \frac{L_{i,m,n}}{T} - D(1 - u_{i,m,n,3}) \tag{24}$$

$$q_{i,m,n}^{out} \leq q_{i,m,n}^{cap} \tag{25}$$

$$q_{i,m,n}^{out} \geq q_{i,m,n}^{cap} - D(1 - u_{i,m,n,4}) \tag{26}$$

$$u_{i,m,n,3} + u_{i,m,n,4} \geq 1 \tag{27}$$

$$u_{i,m,n,3}, u_{i,m,n,4} \in \{0,1\} \tag{28}$$

where $u_{i,m,n,3}$,$u_{i,m,n,4}$ are binary variables.

In addition, equation (16) is replaced by the following three equations:

$$q_{i,m,n}^{cap} \leq w_{i,m}^{c} \mathrm{Q} \tag{29}$$

$$q_{i,m,n}^{cap} \geq w_{i,m}^{c} Q - D(1 - \delta_{i,m,n})\mathrm{Q} \tag{30}$$

$$w_{min}\delta_{i,m,n}\mathrm{Q} \leq q_{i,m,n}^{cap} \leq w_{max}\delta_{i,m,n}\mathrm{Q} \tag{31}$$

F. Objective Function

The cost criterion to be minimized is defined as follows:

$$J = \frac{\sum_{i=1}^{4}\sum_{m=1}^{M}\sum_{n=1}^{N}\frac{T}{2}(L_{i,m,n} + L_{i,m,n-1})}{\sum_{i=1}^{4}\sum_{m=1}^{M}\sum_{n=1}^{N} T \cdot q_{i,m,n}^{in}} + \lambda_1\sum_{i=1}^{4}\sum_{m=1}^{M}\sum_{n=1}^{N}(\delta_{i,m,n} - \delta_{i,m-1,n})^2 + \lambda_2\sum_{i=1}^{4}\sum_{m=1}^{M}(w_{i,m}^{c} - w_{i,m-1}^{c})^2 \tag{32}$$

which is composed of three terms, with the first one being linear and the last two quadratics. The first term represents the average travel delay, and is the kernel term based to evaluate the proposed control actions. The second term penalizes the variation of the control actions in consecutive time steps to ensure as small as possible changes of the green time of each approach i from one control time step to the next in each cycle. In essence, this second term serves to smooth the temporal allocation of road resources over cycles. The third term penalizes the variation of the control actions in consecutive time steps to avoid sharp changes of $w_{i,m}^{c}$ from one cycle to

the next, which aims to smooth the spatial allocation of road resources over cycles.

G. Binary-mixed-integer-quadratic-programing Problem Formulation

The integrated optimal control problem for the traffic signal and internal boundaries under consideration can be written in a compact state-space form as follows:

$$min \quad J = c^T x + \frac{1}{2} x^T H x \tag{33}$$

subject to

$$Ax \leq b \tag{34}$$
$$A_{eq} x = b_{eq} \tag{35}$$
$$v_{lb} \leq x \leq v_{ub} \tag{36}$$
$$x = [x_1{}^T, x_2{}^T]^T,\ x_1 \in \mathbb{R},\ x_2 \in \mathbb{Z} \in \{0,1\} \tag{37}$$

The decision variables x include the state variables at all simulation times of the model, including continuous variables x_1 and binary variables x_2.

$$x_1 = [\underbrace{L_{i,m,n}, q^{cap}_{i,m,n}, q^{out}_{i,m,n}, w^c_{i,m}, w_{i,m}}_{i=1,2,3,4;\ m=1,\dots,M;\ n=1,\dots,N}]^T$$

$$x_2 = [\underbrace{\delta_{i,m,n}, u_{i,m,n,1}, u_{i,m,n,2}, u_{i,m,n,3}, u_{i,m,n,4}}_{i=1,2,3,4;\ m=1,\dots,M;\ n=1,\dots,N}]^T$$

The vector c and matrix H in (33) are determined based on the objective functions (32), where c corresponds to the first term, and H corresponds to the two other quadratic terms. The inequality constraints in (34) correspond to formulae (9), (10), (17)-(31), where matrix A and vector b contain the coefficients in relation to the state variables. Similarly, (35) corresponds to formulae (2)-(8), (14), and matrix A_{eq} and vector b_{eq} correspond to the coefficient relating to state variables. (36) address the bounds of the state variables, including the upper and lower limits of the width ratios and green times, etc.

IV. Simulation Studies

A. Study Setup

The considered isolated intersection with four arms is already shown in Fig. 1. The modelling time step T was set to be 5 s, the cycle length C was 60 s. The considered simulation time horizon was 1 hour, so M and N in (32) were set to be 60 and 12. The total capacity Q of the intersection for the north/south and east/west bound traffic was the same, 9000 veh/h. The large number D used for the constraint linearization in (18), (20), (24), (26), and (30) was $1e^6$.

The upper and lower bounds w_{min} and w_{max} in (11) were 0.15 and 0.85. The lower and upper bounds g_{min} and g_{max} in (1) were 10 s and 50 s. The coefficients in the cost criterion (32) were: $\lambda_1 = 1e^{-2}$, $\lambda_2 = 1e^{-3}$. The proposed optimization problem was solved using the combination of GUROBI and PYTHON on a personal computer with a quad-core processor running at 3.4 GHz with 8 GB memory.

Four control methods were considered for this study: (1) fixed lane-setting and fixed signal timing (Fixed-Fixed); (2) fixed lane-setting and signal timing optimization (Fixed-SGO); (3) internal boundary control and fixed signal timing (IBC-Fixed); (4) internal boundary control and signal timing optimization (IBC-SGO).

Fixed lane-setting means that the internal boundary control wasn't considered and the road resources (the total road width) is distributed evenly for traffic demands in the opposite directions, i.e. between approaches 1 and 3 in Fig. 1. Fixed signal timing means that the total cycle time was equally shared between north/south and east/west bound traffic. IBC means that internal boundary control was considered with the initial lane resource evenly allocated for traffic in the opposite directions. SGO means signal timing optimization was considered with the initial cycle time evenly shared between the opposing traffic.

The control performance evaluation was conducted with respect to three traffic scenarios:

Scenario 1 (Fig. 3): The demands in Approaches 1 and 3 as well as in Approaches 2 and 4 were set equal, but the demands in the opposing directions were not. Clearly, IBC does not work for this scenario, but SGO may suffice.

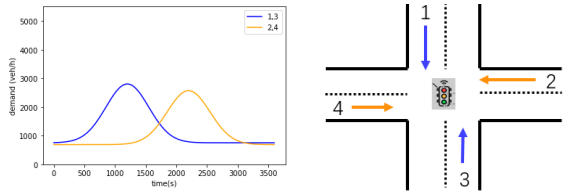

(a) (b)

Fig. 3 Demand profiles for scenario 1.

Scenario 2 (Fig. 4): The demands in the opposite directions (Approaches 1 and 3, 2 and 4) were different, but the largest demands in the opposing directions (the north and west bound traffic) were identical. Clearly, SGO does not work for this scenario, but we wanted to check if IBC alone may suffice.

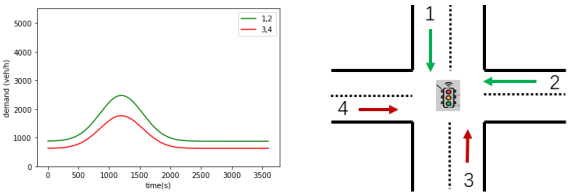

(a) (b)

Fig. 4 Demand profiles for scenario 2.

Scenario 3 (Fig. 5): This scenario was designed such that neither SGO nor IBC alone suffice but the combination of the two can handle the problem.

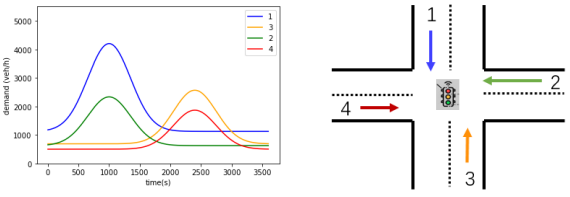

(a) (b)

Fig. 5 Demand profiles for scenario 3.

Four control methods previously introduced were considered for each of the three scenarios. Via the comparative studies for each scenario and across the three scenarios, this paper intends to expose the intrinsic properties of IBC and its potential in combination with SGO for urban traffic optimization.

B. *Scenario 1*

The simulation study results for this scenario are shown in Fig. 6 with the four control methods considered. More specifically, each sub-figure displays the average demand and average capacity allocated for each approach over cycles.

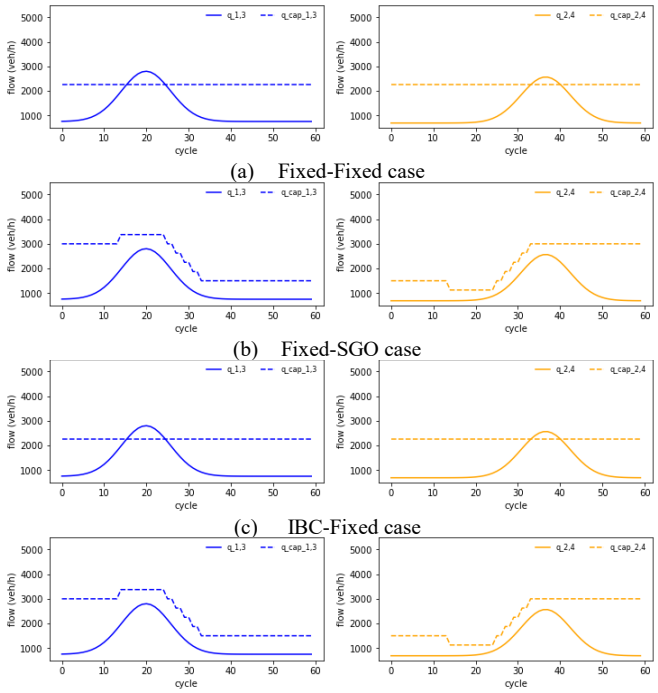

(a) Fixed-Fixed case

(b) Fixed-SGO case

(c) IBC-Fixed case

(d) IBC-SGO case

Fig. 6 Demands and capacities over cycles for scenario 1

Control method 1 (Fixed-Fixed): The time resource was equally allocated for the opposing traffic, so the capacity allocated to Approaches 1 & 3 (Fig. 3) was 1/2*Q (Q=9000 veh/h), and that to Approaches 2 & 4 was also 1/2*Q. Since the road width was equally allocated for traffic in the opposite directions (Fig. 3), the total intersection capacity Q was evenly allocated among the four approaches. As shown by Fig. 3, the total peak demand in Approaches 1 and 3 and that in Approaches 2 and 4 were both higher than 1/2*Q. As such, each approach to the intersection was oversaturated over its peak period. Fig. 6a presents the corresponding results, where the solid curves address the demand in Approach 1/3 and that in Approach 2/4, the dashed lines correspond to 1/4*Q. Approaches 1 and 3 were both oversaturated from the 15th to 25th cycle; at the meantime Approaches 2 and 4 were under-saturated with a lot of spare capacity. The opposite situation happened from the 33th to 39th cycle.

Control method 2 (Fixed-SGO): The total intersection capacity Q was distributed temporally between Approaches 1 & 3 and Approaches 2 & 4, and the resulting capacity allocation was sufficient to meet the demands in all approaches, see Fig. 6b, where the dashed lines represent the distributed capacities via signal optimization. Note that the sum of the two dashed curves in Fig. 6b for any cycle is equal to 1/2*Q.

Control method 3 (IBC-Fixed): As the demands in any two opposite directions were the same, the IBC was not supposed to work, and this was confirmed with Fig. 6c, which is exactly the same as Fig. 6a.

Control method 4 (IBC-SGO): For the same reason as illustrated with Figs. 6a and 6c, the results from this case should be the same as those in Fig. 6b (Fixed-SGO), see Fig. 6d.

The reader is also referred to Table 1 for the performance comparison of the four control methods with respect to scenario 1.

C. *Scenario 2*

As discussed before, the following is expected for the control results with this scenario (Fig. 4): (1) the initially equal allocation of time resources for the south and west bound traffic is proper, and SGO would make no difference; (2) unbalanced traffic demands in the opposite directions determines the IBC would make some difference. Also, it is anticipated that the Fixed-Fixed case and the Fixed-SGO case have the same results, and the IBC-Fixed and IBC-SGO cases have the same results. All these were confirmed with Fig. 7.

It is noted that the two dashed curves in Figs. 7c refer to the allocated capacity for traffic in the corresponding approaches, and the sum of them is equal to 1/2*Q for any cycle. Clearly, the demand in each approach was satisfied by the allocated capacity. The reader is also referred to Table 1 for a summary.

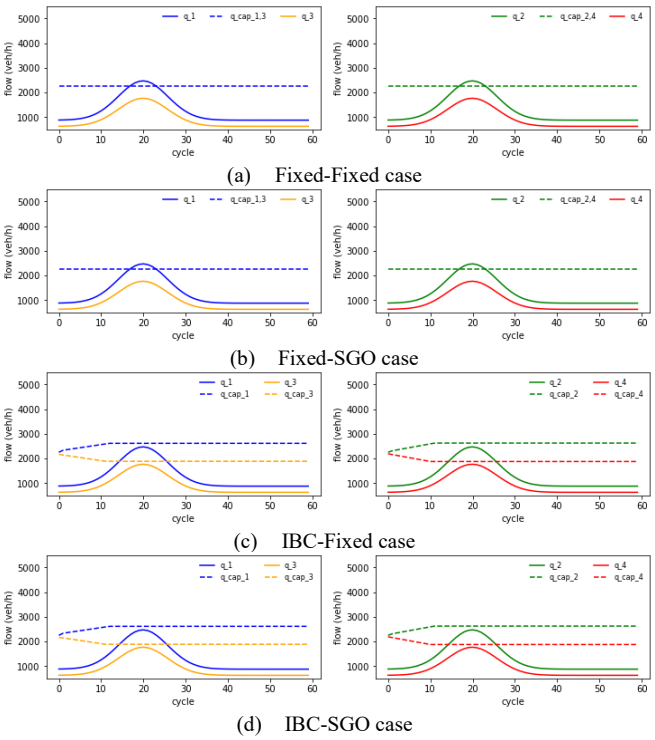

(a) Fixed-Fixed case

(b) Fixed-SGO case

(c) IBC-Fixed case

(d) IBC-SGO case

Fig.7 Demands and capacities over cycles for scenario 2

D. *Scenario 3*

This scenario (Fig. 5) was designed such that both SGO and IBC would be significant.

The study results are presented in Fig. 8. Firstly, purely the SGO case (Fig. 8b) could not accommodate the traffic demands in approaches 1 and 2. Secondly, purely IBC (Fig. 8c) was not able to fully handle the demand in approach 1. Thirdly, the integrated IBC and SGO satisfactorily tackled the problem. Note that the total capacity in Fig. 8b (the sum of the two

dashed curves in two sub-figures for any cycle) is equal to 1/2*Q, the total capacity in Fig. 8c (the sum of the two dashed curves in each sub-figure for any cycle) is equal to 1/2*Q, and the total capacity in Fig. 7d (the sum of the fourth dashed curves for any cycle) is equal to Q. Fig. 9 displays the total number of queueing vehicles from all approaches for each cycle, the reader is also referred to Table 1 for a summary.

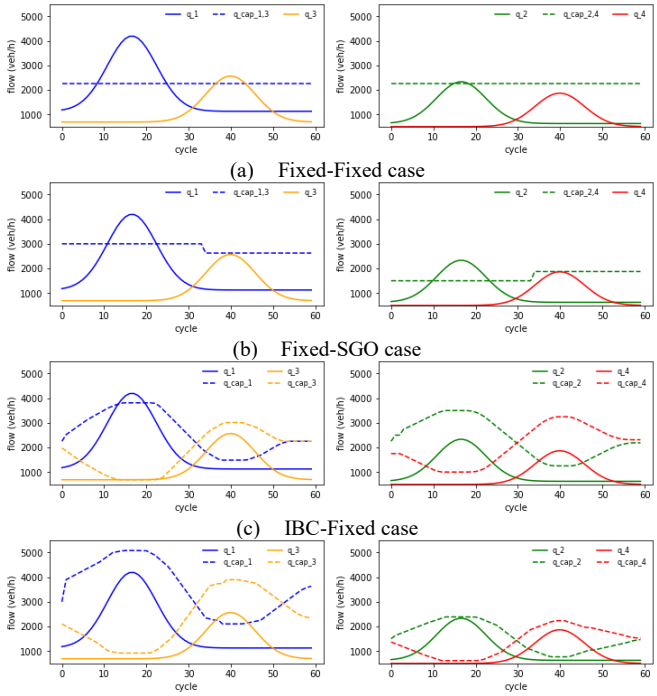

(a) Fixed-Fixed case

(b) Fixed-SGO case

(c) IBC-Fixed case

(d) IBC-SGO case

Fig. 8 Demands and capacities over cycles for scenario 3.

TABLE I. THE PERFORMANCE FOR THREE SCENARIOS

Performance	Scenario 1	Scenario 2	Scenario 3	
	Average Delay	*Average Delay*	*Average Delay*	*Max Queue*
Fixed-Fixed	27.21	13.39	92.31	362.95
Fixed-SGO	10.03 (-63.1%)	13.39 (0%)	52.12 (-43.54%)	304.44 (-16.12%)
IBC-Fixed	27.21 (0%)	10.88 (-18.7%)	12.95 (-85.97%)	85.64 (-76.40%)
IBC+SGO	10.03 (-63.1%)	10.88 (-18.7%)	10.09 (-89.07%)	58.64 (-83.85%)

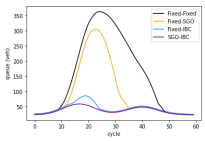

Fig. 9 Queue over cycles for scenario 3.

V. CONCLUSION

The possibility of regulating urban roads' internal boundaries between opposite directions is investigated for lane-free traffic of connected automated vehicles. Particularly, the coordinated optimization of internal boundaries and signal timing for an isolated intersection has been studied. The optimization task problem is formulated as a binary-mixed-integer-quadratic-programing problem and solved using the standard branch-and-bound technique. The obtained results show that the joint optimization can better deal with traffic situations at an intersection, particularly those not tractable via signal timing optimization alone. Signal timing optimization can be applied to allocate the road capacity temporally to address unbalanced incompatible traffic demands in the opposing directions, while the internal boundary control assigns the road capacity spatially to deal with unbalanced compatible traffic demands in the opposite directions. The two control measures are both significant and irreplaceable. The co-utilization of both measures leads to the traffic efficiency improvement that either measure alone cannot achieve. Further studies will consider left-turning movements, regulatable cycles, and multiple intersections.

REFERENCES

[1] G. Improta and G. E. Cantarella, "Control system design for an individual signalized junction," Transportation Research. Part B: Methodological, vol. 18, (2), pp. 147-167, 1984.

[2] J. Li, "Discretization modeling, integer programming formulations and dynamic programming algorithms for robust traffic signal timing," Transportation Research. Part C, Emerging Technologies, vol. 19, (4), pp. 708-719, 2011.

[3] J. Zhao, Y. Liu and X. Yang, "Operation of signalized diamond interchanges with frontage roads using dynamic reversible lane control," Transportation Research. Part C, Emerging Technologies, vol. 51, pp. 196-209, 2015.

[4] J. Wojtowicz and W. A. Wallace, "Traffic management for planned special events using traffic microsimulation modeling and tabletop exercises," Journal of Transportation Safety & Security, vol. 2, (2), pp. 102-121, 2010.

[5] C. Xie and M. A. Turnquist, "Lane-based evacuation network optimization: An integrated Lagrangian relaxation and tabu search approach," Transportation Research. Part C, Emerging Technologies, vol. 19, (1), pp. 40-63, 2011.

[6] A. Karoonsoontawong and D. Lin, "Time-Varying Lane-Based Capacity Reversibility for Traffic Management: Lane-based capacity reversibility for traffic," Computer-Aided Civil and Infrastructure Engineering, vol. 26, (8), pp. 632-646, 2011.

[7] Z. Di and L. Yang, "Reversible lane network design for maximizing the coupling measure between demand structure and network structure," Transportation Research. Part E, Logistics and Transportation Review, vol. 141, 2020.

[8] C. K. Wong and S. C. Wong, "Lane-based optimization of signal timings for isolated junctions," Transportation Research. Part B: Methodological, vol. 37, (1), pp. 63-84, 2003.

[9] C. K. Wong and B. G. Heydecker, "Optimal allocation of turns to lanes at an isolated signal-controlled junction," Transportation Research. Part B: Methodological, vol. 45, (4), pp. 667-681, 2011.

[10] C. Yu et al, "Robust Optimal Lane Allocation for Isolated Intersections: Robust optimal lane allocation," Computer-Aided Civil and Infrastructure Engineering, vol. 32, (1), pp. 72-86, 2017.

[11] M. Papageorgiou et al, "Lane-Free Artificial-Fluid Concept for Vehicular Traffic," Proceedings of the IEEE, vol. 109, (2), pp. 114-121, 2021.

[12] M. Malekzadeh et al, "Optimal internal boundary control of lane-free automated vehicle traffic," Transportation Research. Part C, Emerging Technologies, vol. 126, 2021.

[13] M. Malekzadeh, I. Papamichail and M. Papageorgiou, "Linear–Quadratic regulators for internal boundary control of lane-free automated vehicle traffic," Control Engineering Practice, vol. 115, 2021.

[14] M. Malekzadeh, I. Papamichail and M. Papageorgiou, " Overlapping internal boundary control of lane-free automated vehicle traffic," Control Engineering Practice, vol. 133, 2023.

[15] X. Jin et al., "Integrated Control of Internal Boundary and Ramp Inflows for Lane-free Traffic of Automated Vehicles on Freeways," 2022 IEEE 25th International Conference on Intelligent Transportation Systems (ITSC), Macau, China, 2022, pp. 1234-1239.

[16] K. Ampountolas, J. A. dos Santos and R. C. Carlson, "Motorway Tidal Flow Lane Control," IEEE Transactions on Intelligent Transportation Systems, vol. 21, (4), pp. 1687-1696, 2020.